OPTIDICER REDUCES LONG CUG RNA ACCUMULATION IN CORNEAL ENDOTHELIAL CELLS FROM PATIENTS WITH FUCHS' DYSTROPHY

by

SANJANA CAROLINE BASAK

A THESIS

Presented to the Department of Biology
and the Robert D. Clark Honors College
in partial fulfillment of the requirements for the degree of
Bachelor of Science

June 2024

An Abstract of the Thesis of

Sanjana C. Basak for the degree of Bachelor of Science
in the Department of Biology to be taken June 2024

Title: Optidicer Reduces Long CUG RNA Accumulation in Corneal Endothelial Cells From Patients With Fuchs' Dystrophy

Approved: *Balamurali K. Ambati, M.D., Ph.D.*
Primary Thesis Advisor

This study will examine the viability of the modified endonuclease, known as OptiDicer, in preventing corneal endothelial cell loss and halting the progression of late-onset Fuchs' Endothelial Corneal dystrophy (FECD). FECD is a debilitating, heritable disease that could impact 415 million people by the year 2050 (Aiello et al., 2022). The consequences of this disease are significant and include loss of vision, painful corneal edema, and collagen excrescences. The current treatment for FECD involves surgical transplantation of donor corneas. This treatment is limited in its capability due to high costs, high transplant rejection and infection rates, and painful long recuperation periods. Developing a targeted gene therapy such as OptiDicer could provide a watershed medical care advancement for patients suffering from late-onset FECD.

This disease manifests from a progressive decrease in corneal endothelial cell density. Prior research indicates that a trinucleotide expanded repeat mutation in the TCF4 gene affects diseased corneal endothelial cells. The excessive repetition of the CTG nucleotide in this gene leads to the overproduction of CUG RNA in the cell nucleus. The overabundance of RNA forms distinct structures, or foci, which are toxic to the corneal endothelial cells. Our treatment,

OptiDicer, is a modified form of the endogenous protein DICER1 that cleaves CUG RNA in cell nuclei via RNase III activity. Unlike DICER1, OptiDicer is miRNA-resistant and can continuously cleave accumulated CUG RNA foci. We expect that OptiDicer will significantly reduce CUG RNA foci in corneal endothelial cell nuclei and prevent endothelial cell death in the cornea.

Acknowledgements

I'd like to thank the members of the Ambati Lab: Dr. Hiro Uehara, Dr. Sangeetha Ravi-Kumar, Bonnie Archer, Kieley Trempy, Baila Shakaib, Saumya Keremane, and Dr. Bala Ambati. Working and learning from this team for over 3 years has been the highlight of my college experience. I'd like to give special thanks to Hiro for being a wonderful mentor; he believed in my potential and gave me a chance to prove myself as a researcher in training. Interacting with Hiro, Sangeetha, and the rest of the Ambati lab inspired me to pursue a biomedical PhD and dedicate my career to research. I'm incredibly lucky to have found such a welcoming, kind, supportive, and talented group of scientists in my time at UO.

I am dedicating this thesis to my parents, Gloria and Indranil Basak. Their loving support has allowed me the freedom in college to explore my interests and pursue my ambitions. I'm so grateful to have them as my family and to celebrate this moment in my life with them.

This thesis would not be possible without the snuggles provided by my best buddy and darling shih tzu, Opus Basak.

Table of Contents

List of Figures

INTRODUCTION

Late-onset Fuchs' endothelial corneal dystrophy (FECD) is a heritable degenerative disorder that is characterized by progressive vision loss and corneal edema. FECD has been demonstrated to be prevalent in Caucasian and Asian populations in adults aged sixty years or older (Mootha et al., 2015; Jurkunas et al., 2010). The disorder has been documented in 11% of females and 7% of males in Reykjavik, Iceland, 8.5% of Chinese Singaporeans, 5.5% of Japanese citizens, and 5% of Caucasians older than 40 years in the United States (Mootha et al., 2015). In the U.S., 14,153 keratoplasties out of 72,736 total corneal transplants in 2013 were performed to treat Fuchs' dystrophy (Xing et al., 2014). In 2022, Fuchs' dystrophy and endothelial dysfunction accounted for 28,143, or 59.7%, of the keratoplasty procedures performed in the U.S. (Mathews et al., 2023). With FECD projected to impact 415 million people globally by 2050, patients and practitioners would greatly benefit from novel treatments for this disorder (Aiello et al., 2022).

Cornea Physiology and FECD Pathology

Fuchs' dystrophy is a corneal disease that manifests from a dysfunctional corneal endothelium. Composed of three cellular layers (epithelium, stroma, and endothelium) and two acellular layers (Bowman's and Descemet's membranes), the transparent cornea regulates vision quality by focusing images on the retina (Faye et al., 2021). The outermost cellular layer, the epithelium, is constructed as a multilayered epithelial sheet of self-renewing cells that continue to achieve mitosis (Sheerin et al., 2012). The stroma is a cellular layer below the epithelium, structured as a lattice of collagen and proteoglycans maintained by keratocytes (Sheerin et al., 2012). The innermost cellular layer is the endothelium, a terminally differentiated cell monolayer

that separates the cornea from aqueous humour (aqueous fluid) (Sheerin et al., 2012). Due to the absence of growth factors in the aqueous humor, corneal endothelial cells are unlikely to enter mitosis and initiate self-regeneration (Sheerin et al., 2012).

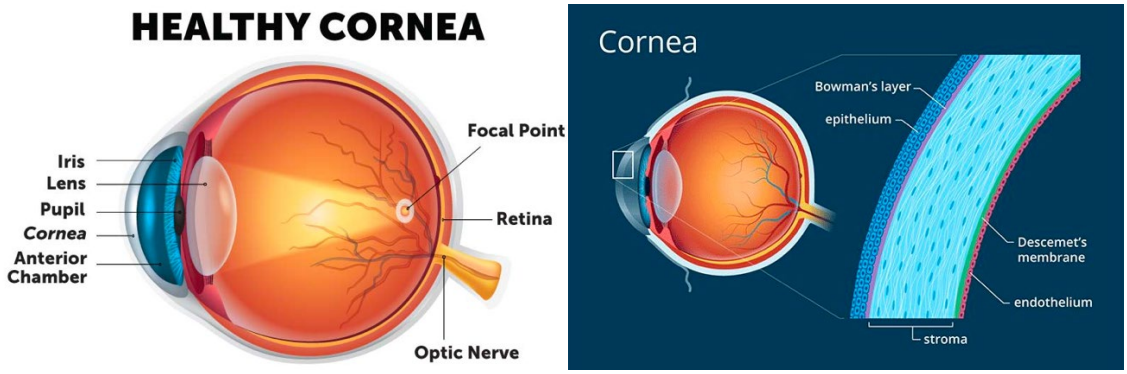

Fig 1: Human Eye and Cornea Physiologies.

A functional corneal endothelium maintains a cell density of 400-500 cells per square millimeter (Sarnciola et al. 2019). The cells are connected at their apical surfaces by tight junctions and joined to adjacent cells by gap junctions (Haschek et al. 2002). The endothelial cells regulate corneal hydration, thickness, and transparency by pumping aqueous fluid between the stroma and the anterior chamber of the cornea (Nanda et al., 2019). Aqueous fluid is pumped into the stroma to facilitate the active transport of nutrients (Sheerin et al., 2012). In contrast, aqueous fluid is pumped out of the stroma so the structure can attain a state of dehydration or deturgescence to maintain corneal transparency (Nanda et al., 2019). The movement of aqueous fluid between the stroma and anterior chamber is mediated by sodium-potassium (Na^+/K^+) and bicarbonate anion-activated ATPase pumps located in the outer endothelial cell membrane (Haschek et al. 2002).

The progressive loss of corneal endothelial cell density and alterations in underlying cellular mechanisms inform the pathology of Fuchs's dystrophy. An FECD patient's corneal endothelium experiences dysregulated senescence (cell cycle arrest), which expedites apoptosis or programmed cell death (Xing et al., 2014). As increased cell death occurs, the unaffected endothelial cells cannot enter mitosis and self-renew due to their terminally differentiated state. Instead, the remaining cells migrate to cover low-density areas in the endothelium (Mootha et al. 2015). The remaining corneal endothelial cells also experience morphological changes such as thinning, stretching, and enlargement (Jurkunas et al., 2010). Cell size and shape changes, or *polymegethism* and *pleomorphism*, disrupt endothelial cells' wild-type hexagonal morphology (Jurkunas et al., 2010). When the cell density becomes too low to be corrected by malformed migratory cells, the corneal endothelium loses its pumping function, and excess aqueous fluid overhydrates the stroma (Hamill et al., 2013). Dysregulated stromal hydration results in corneal opacity, edema, scarring, and reduced vision (Hamill et al., 2013).

An additional pathological marker of FECD is *guttae* formation near the endothelium. Descemet's membrane, located directly below the endothelium, becomes diffusely thickened with FECD progression (Mootha et al., 2015). The thickened membrane induces the formation of focal collagenous excrescences, known as *guttae* (Mootha et al., 2013). Guttae formation and corneal endothelial cell loss are initiated in the central cornea and progress to the periphery of the tissue (Jurkunas et al., 2010). Through visualizing the mound-shaped collagenous excrescences with slit lamp biomicroscopy, studies suggest the number of endothelial cells remaining in the cornea is inversely proportional to the number of guttae (Jurkunas et al., 2010).

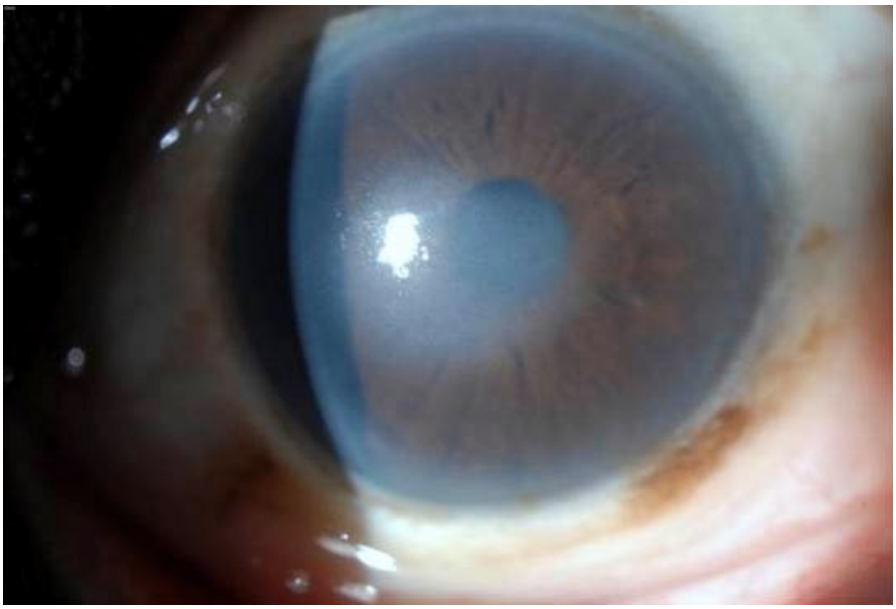

Fig 2: Patient with advanced Fuchs' dystrophy.

FECD Genetic Markers and Underlying Mechanisms

Late-onset FECD is a disorder with locus heterogeneity and multiple genetic markers not integrated into a cohesive pathology (Mootha et al., 2015). While smoking and low body mass index have been implicated as potential FECD risk factors, environmental risk factors have not been found to inform FECD pathogenesis (Wieben et al., 2012). Prior studies describe the disorder as an autosomal-dominant trait transmitted through generations (Hamill et al., 2013). However, late-onset Fuchs' dystrophy has been demonstrated to exhibit incomplete penetrance and phenocopies in large pedigrees (Mootha et al., 2015). In other words, individuals who carry the FECD variant gene may not phenotypically exhibit the disorder, while individuals with the disorder may not carry the FECD gene variant. The gene variants discussed in this paper include TCF8, LOXHD1, and TCF4, in addition to current data on RNA-mediated toxicity, aberrant splicing, differential mitochondrial activity, and oxidative stress implicated in late-onset FECD pathogenesis.

In a minority of late-onset FECD cases, the development of the disorder is attributed to mutations in the TCF8 and LOXHD1 loci. TCF8 encodes ZEB1, a zinc-finger transcription factor family protein with gene-repressive and enhancive capabilities (Hamill et al. 2013). TCF8 expression in the corneal endothelium is presumed to regulate epithelial-mesenchymal transition or the process of epithelial cells obtaining migratory properties and becoming mesenchymal stem cells (Hamill et al. 2013). Five loss-of-function mutations in the TCF8 gene on chromosome 10 may contribute to the development of FECD (Hamill et al., 2013). Another genetic marker documented in a minority of late-onset FECD cases is a mutation in the LOXHD1 gene on chromosome 18 (Hamill et al., 2013). LOXHD1 encodes a protein consisting of PLAT domains and is suspected of regulating protein interactions in the plasma membrane (National Library of Medicine). FECD patients have exhibited LOXHD1 mutations, which overexpress the LOXHD1 protein in the cornea (Hamill et al., 2013). High levels of LOXHD1 have been observed to result in cytotoxic aggregations, which could contribute to corneal endothelial cell loss and FECD pathogenesis (Hamill et al., 2013).

The gene variant found in 70% of FECD cases in the United States is a repeat-expansion mutation in the transcription factor 4 (TCF4) locus on chromosome 18 (Hu et al., 2018). In 2010, Baratz et al. conducted a genome-wide association study (GWAS) that indicated a correlation between the single nucleotide polymorphism (SNP) rs613872 in the TCF4 gene and late-onset FECD. Subsequently, in 2012, Wieben et al. demonstrated that a cytosine-thymine-guanine (CTG) repeat in intron 3 of TCF4 had greater specificity as a FECD genetic marker. The Wieben et al. study reported that 52 of 66 FECD subjects had the expanded CTG alleles, while only 2 of 63 controls displayed this genotype (Mootha et al., 2013). These findings agreed with a 1997 study by Breschel et al., which identified the intronic trinucleotide repeat locus, termed

CTG18.1, as a statistically significant genetic marker in a Caucasian cohort (Mootha et al., 2013). The TCF4 gene extends over 437 kb on chromosome 18 and includes 20 exons (Du et al., 2015; Mootha et al., 2013). The gene gives rise to 48 different transcripts from more than 20 mutually exclusive transcription start sites (Du et al., 2015). TCF4 encodes for E2-2, a 667-amino acid, class I, basic helix-loop-helix transcription factor that binds to the canonical E-box sequence CANNTG of promoters of target genes (Mootha et al., 2013; Mootha et al., 2015).

Studies conducted by Breschel et al., Wieben et al., Du et al., and Mootha et al. have implicated expanded CTG18.1 alleles of n>30-40 repeats to be present in late-onset FECD patients. A copy of the expanded CTG18.1 allele confers a more than 32-fold increased risk of developing late-onset FECD (Mootha et al., 2013). Despite the evidence identifying the expanded CTG18.1 allele as a risk factor, the mechanisms contributing to corneal endothelial degeneration and FECD development are unknown. Potential mechanisms of the CTG repeat mutation in FECD may include RNA-mediated toxicity, haploinsufficiency of TCF4, or an unsuspected mechanism (Mootha et al., 2015). RNA-mediated toxicity is a strong contender in FECD pathogenesis since the expanded CTG18.1 allele is located in an intron; no protein product is ultimately translated from this non-coding region (Du et al., 2015). In other repeat-expansion diseases such as myotonic dystrophy 1 and 2 (DM1 and DM2), expanded microsatellite DNA sequences are also located in non-coding intronic regions (Du et al., 2015). In DM1 pathogenesis, CTG repeats are transcribed into poly(CUG)$_n$ mRNA (Du et al., 2015). The DM1 RNA transcripts with expanded CUG repeats form stable hairpin structures, which interact and sequester RNA binding proteins and induce degenerative molecular pathways (Mootha et al., 2015). The hairpin RNA structures, denoted as *foci,* further exhibit cytotoxic, gain-of-function activity by stimulating misplicing events and apoptosis (Mootha et al., 2015).

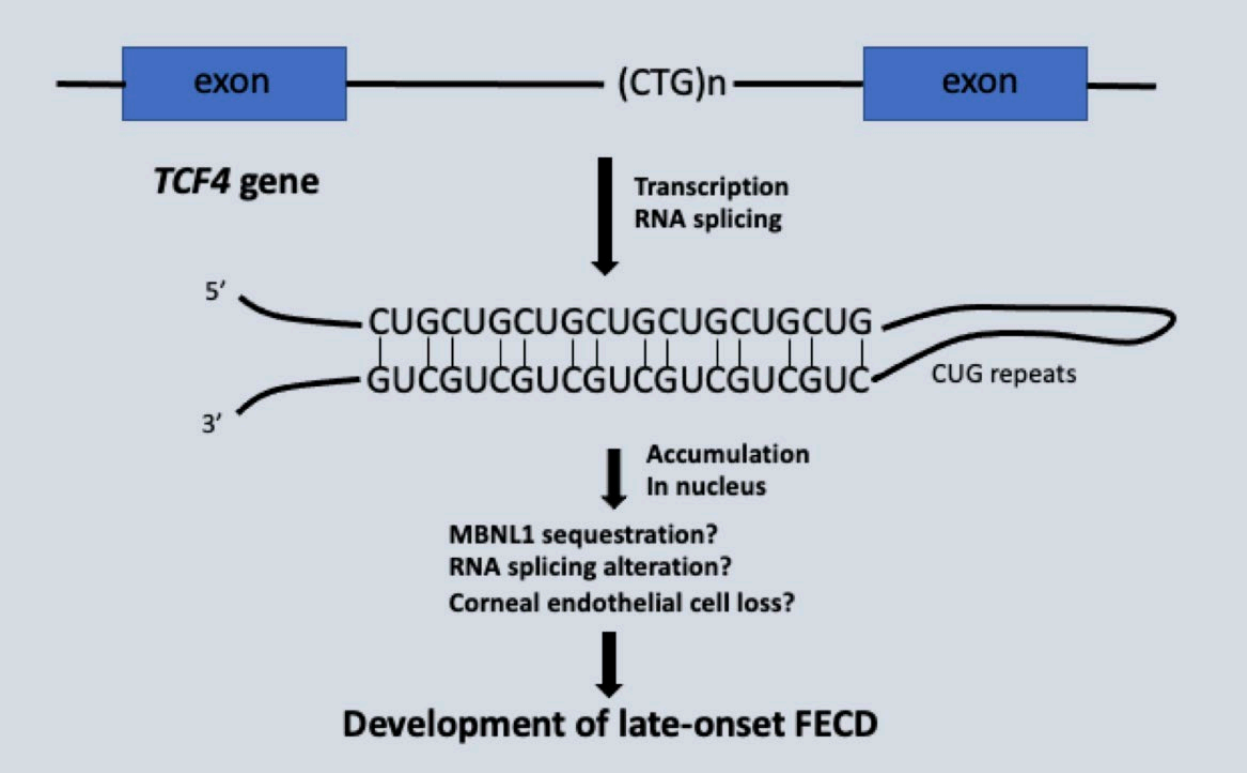

Fig. 3: Long (CTG)n repeat (n>30-40) in TCF4 is associated with FECD.

Mootha et al. and Du et al. demonstrate that, similarly to DM1, ribonuclear foci can be detected in late-onset FECD corneal endothelial cells. A 2015 study identified discrete nuclear RNA foci of variable size in all eight endothelial samples of FECD subjects with CTG18.1 expansion (Mootha et al., 2015). Nuclear RNA foci were undetectable in five control endothelial samples without the expansion, while two control samples with ribonuclear foci were found to have mutant CTG18.1 alleles (Mootha et al., 2015). The average percentage of cells with nuclear RNA foci in the eight CTG18.1 expansion-positive FECD endothelial samples ranged from 33% to 88% (Mootha et al., 2015). The observed morphology of the foci was spheroidal, and foci size ranged from 0.43 to 2.59 μm^2 (Mootha et al., 2015). While Mootha et al. observed a range of 0.39 to 1.55 average foci per cell nucleus, Du et al. reported 2.35 ± 1.14 foci per cell nucleus.

When the pathology of late-onset FECD is compared to DM1 again, poly(CUG)$_n$ RNA in DM1 co-localizes with and sequesters the mRNA-splicing factor MBNL1 (Du et al., 2015). Sequestration of MBNL1 disrupts the splicing of MBNL1-regulated mRNAs, such as the chloride channel ClC-1 and the insulin receptor (Du et al., 2015). Du et al. demonstrate in their 2015 study that two FECD patients with CTG18.1 expansion exhibited co-localization of CUG RNA foci and MBNL1 protein, while CUG RNA foci and MBNL1 aggregation were not detected in a CTG18.1 expansion-negative FECD patient. Further investigation by Du et al. on potential CUG RNA foci interference with splicing factors revealed that 342 genes with robust expression in the corneal endothelium had differential expression of at least one isoform in FECD samples. Top differential splicing events identified by Du et al. involved MBNL1 and the MBNL1-regulated genes ADD3 and INF2. Implementation of MISO (Mixture of Isoforms) software by Du et al. provided estimates of isoform expression at the exon level. MISO analysis of MBNL1 splicing in CTG18.1 expansion-positive FECD samples revealed that the inclusion of exon 6 (352-bp band) of MBNL1 is more highly favored in FECD patients than in the control (Du et al., 2015). MBNL1 splicing in a control sample resulted in two strong PCR products with sizes of 352-bp and 298-bp, while an FECD sample resulted in a strong 352-bp product and very little of the 298-bp product (Du et al., 2015). Similarly, analysis of splicing of the gene product ADD3 indicated that the inclusion of exon 14 (380-bp band) is favored in CTG18.1 expansion-positive FECD samples (Du et al., 2015). In contrast, control samples for ADD3 splicing exhibit a robust 298-bp PCR product and little of the 380-bp PCR product (Du et al., 2015). Lastly, splicing analysis for the INF2 gene product demonstrates preferential exclusion of exon 22 (352-bp band) (Du et al., 2015). The 352-bp PCR product shows up strongly in control samples, but only CTG18.1 expansion-positive samples exhibit a 295-bp PCR product (Du et al., 2023). The

differential splicing events in MBNL1 and MBNL1-regulated ADD3 and INF2 transcripts support previous findings that CUG RNA foci in CTG18.1 expansion-positive FECD cells sequester MBNL1 and induce aberrant splicing. Furthermore, ADD3 and INF2 proteins are suspected to be involved in actin dynamics within cells and cell-cell adhesion (Du et al., 2015). Dysregulated splicing of these proteins involved in mechanical support and movement of cells may contribute to corneal endothelial cell death and late-onset FECD pathogenesis.

Current literature emphasizes the role of CTG18.1 expansion, RNA-mediated toxicity, and differential splicing in FECD pathogenesis. However, multiple studies demonstrate that dysregulated mitochondrial activity and oxidative stress may be critical in FECD development. Corneal endothelial cells are highly populated with mitochondria, which are cell organelles that generate chemical energy via oxidative phosphorylation (Haschek et al. 2002). A robust mitochondrial presence is necessary for endothelial cells to maintain corneal hydration, thickness, and transparency (Nanda et al., 2019). The bicarbonate anion-activated ATPase located within mitochondria allows endothelial cells to perform the metabolically costly activity of pumping stromal fluid into the anterior chamber of the cornea (Haschek et al. 2002). The progression of FECD may be correlated with increased oxidative stress in corneal endothelial cells due to an inefficient mitochondrial system (Nanda et al. 2019). FECD cells have been found to have increased mitochondrial DNA damage, decreased mitochondrial membrane potential, and mitochondrial fragmentation (Nanda et al. 2019). Jurkunas et al. further report that a marker of oxidative DNA damage, 8-hydroxy-2’-deoxyguanosine, co-localizes to mitochondria in FECD samples, demonstrating that the mitochondrial genome is the specific target of oxidative stress in FECD. A promising avenue for FECD gene therapy could be preventing the decline of

mitochondrial mass and correcting the oxidant-antioxidant imbalance in corneal endothelial cells.

Current and Future Treatments for FECD

Current treatments for late-onset Fuchs' dystrophy are solely surgical. Penetrating Keratoplasty (PKP) has become outdated in FECD treatment practice due to its extensive recovery period, permanent weakening of tectonic eye strength, high rates of transplant rejection, and serious risk of suture infection (Sarnicola et al. 2019). Endothelial Keratoplasty, the current standard for late-onset FECD treatment, has improved upon the failures of PKP and results in faster recovery, rescued vision loss, and low transplantation rejection (Sarnicola et al. 2019). However, with FECD cases on the rise, the need for quality corneal transplant tissue has outpaced the supply chain.

The global cornea donor shortage has provided a prime opportunity to position a genetic therapy in FECD care. Our treatment, OptiDicer, is a modified endonuclease that aims to treat FECD by continuously cleaving CUG RNA accumulations and preventing the formation of cytotoxic RNA foci. OptiDicer is a modified form of the endogenous protein DICER1 responsible for degrading miRNA and mRNA via RNase III activity. In contrast to DICER1, OptiDicer does not respond to negative feedback and can cleave accumulated CUG RNA continuously. Removal of the helicase domain in OptiDicer allows RNase III activity to occur unchecked. We expect that OptiDicer will significantly reduce CUG RNA accumulations in corneal endothelial cell nuclei and rescue corneal endothelial cell death by preventing RNA-mediated toxicity, sequestration of MBNL1, and dysregulated splicing.

METHODS

OptiDicer Design and Plasmid Construction

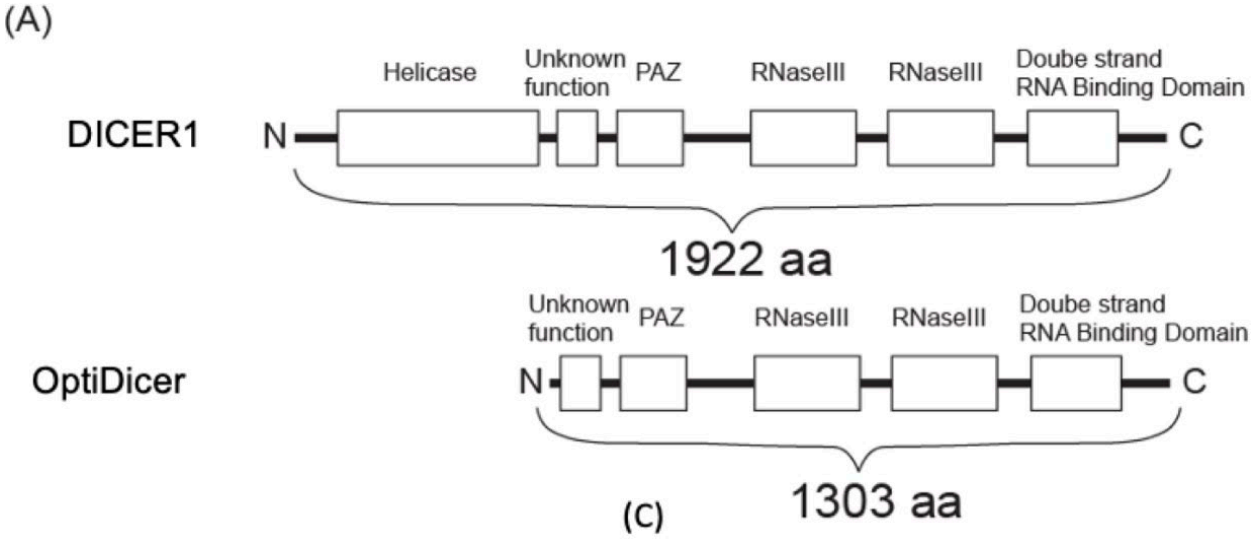

Fig 4: Comparison of OptiDicer modifications and endogenous DICER1.

OptiDicer was initially developed by Dr. Hironori Uehara to prevent retinal pigmented epithelial cell loss in Geographic Atrophy. The original sequence of OptiDicer was posted in GenBank as MN910264. Endogenous DICER1consists of a helicase domain, PAZ domain, two RNase III domains, and a DRBM domain and has a full length of 5.8 kb. Previous studies demonstrate that the N-terminus helicase domain has an inhibitory effect on DICER1 double-strand RNA cleavage (Ma et al., 2008). The N-terminus helicase domain was removed to optimize RNA cleavage efficiency and reduce dicer's size. To package DICER1 into an adeno-associated virus (AAV) for transfection, the promoter and polyadenylation signal were modified to reduce the dicer packaging size to ~5.0kb. In addition to the N-terminus helicase domain, miRNA production via DICER1 cleavage is also suspected to have an inhibitory function by inducing a negative feedback loop. OptiDicer was modified to be resistant to let-7 miRNA with silent mutations on let-7 target regions (DNA sequence changes, but not protein sequence). The

negative feedback loop stimulated by miRNA production was further corrected by removal of all potential miRNA targeting sites. Since mature miRNA is ~22 nt, the seed sequence was reduced to ~7 nt to only recognize target mRNA. miRDB (http://mirdb.org/miRDB/index.html) was used to alter the seed miRNA sequence of OptiDicer with silent mutations. Lastly, NLS-OptiDicer was given a nuclear localization signal (NLS) for expression in cell nuclei only. We introduced NLS at the N-terminus, C-terminus, and both termini. We found C-terminus NLS decreased OptiDicer expression. Therefore, NLS-OptiDicer was modified to contain c-myc derived NLS (PAAKRVKLD) at the N-terminus.

Cell culture

The patient derived FECD corneal endothelial cells F35T (>1500 CTG repeats) were a generous gift from Dr. Albert Jun. Cells were cultured in "Joyce" medium designed by Dr. Nancy C. Joyce. The Joyce medium consisted of 2% fetal bovine serum, 8% chondroitin sulfate (C9819), P/S/A (anti-anti), BPE (pituitary extract) (Gibco, 13028-014), 100mg/mL CaCl2, 10mg/mL ascorbic acid (A4403), and 100µg/mL EGF, and OptiMEM (1x)/GlutaMAX (Gibco). When cells achieved confluence in Joyce media, the media was changed to human corneal endothelial maturation medium (Gibco).

Immunofluorescence

Cells were plated in an 8-well chamber slide with FNC coating at 0.05 x 106 cells/well. The cells were incubated overnight at 37°C, and transfection was performed with Lipofectamine3000 Transfection Reagent (Thermofisher). The protocol involved diluting 0.25ug AAV plasmid, 0.375 µL Lipofectamine3000, and 0.5µL P3000 with 25µL OptiMEM (1X)/GlutaMAX. After 10

minutes of incubation, 25µL of diluted transfection solution was added dropwise to a well containing 250µL of Joyce medium. Joyce medium was changed after 24 hours of incubation.

After washing cells twice with 1X PBS, 500µL of 4% PFA was used to fix cells for 15 minutes. Following a triple-wash with 70% RNase-free ethanol, 500µL of 70% EtOH was permeabilized in each well for 30 minutes at 4°C. Cells were washed twice with 1x PBS and blocked with 5% FBS, 0.02% triton, and 1x PBS for 60 minutes at room temperature. The meniscus of the 8-well chamber slide was removed, and wells were washed with a blocking buffer. The cells were incubated with 50µL of Dicer rabbit monoclonal primary antibody (D38E7, 1:100) dispersed dropwise. Cells were placed overnight in a humidified incubation tray at 4°C.

Cells were washed with 1X PBST (0.01% T detergent) 6 times for 10 minutes. Afterward, they were incubated with 100µL Alexa Fluor goat anti-rabbit IgG HRP secondary antibody (1:500, Thermofisher) for 1-2 hours at room temperature. The PBST wash regimen was repeated, and cells were stained with mounting media with DAPI. The cells were imaged with an EVOS fluorescence microscope at 10X and 40X magnification.

Western blot

Cells were plated in a 24-well plate with FNC coating at 0.1 x 106 cells/well. The cells were incubated overnight at 37°C, and transfection was performed with Lipofectamine3000 Transfection Reagent (Thermofisher). The protocol involved dilution of 0.5µg AAV plasmid, 0.75µL Lipofectamine3000, and 1µL P3000 with 50µL OptiMEM (1X)/GlutaMAX. After 10 minutes of incubation, 50µL of diluted transfection solution was added dropwise to a well containing 500µL of Joyce medium. Joyce medium was changed after 24 hours of incubation, and the cells were incubated for 48 hours.

Following a double wash with cold PBS, 200µL of RIPA buffer and protease inhibitor was dispensed to each well and incubated for 30 minutes on ice. The cells were collected with a cell scraper and lysed by centrifugation at 12,000g for 5-10 minutes. The supernatant was collected, and protein concentration was ascertained with a BCA protein assay kit. A buffer comprised of 10% BME and 4X LDS (Invitrogen NuPAGE) was added to each sample and the samples were incubated for 10-15 minutes at 70°C. Equal amounts of protein were loaded onto 4-12% Bis-Tris 10-well polyacrylamide gels (Invitrogen NuPAGE) and transferred onto PVDF membranes. Westerns were performed with 1X MOPS and 10% MeOH 1X transfer buffer (20X transfer buffer, RO water, 100% MeOH). Protein samples were incubated with Dicer rabbit monoclonal primary antibody (D38E7, 1:500) and Alexa Fluor goat anti-rabbit IgG HRP secondary antibody (1:2000, Thermofisher) in 3% blocking buffer (milk powder, 1X PBST). The gel images were obtained by Azure Biosystems™ c280 (Azure Biosystems).

Fluorescent in situ hybridization (FISH)

Cell plating and transfection occurred as previously described in the immunofluorescence protocol. After washing with 1X PBS, cells were fixed with 500 µL 4% PFA for 30 minutes at room temperature. Cells were washed twice with 70% EtOH and permeabilized with 500 µL 70% EtOH overnight at 4°C. The following day, cells were washed with wash buffer (10% formamide in 0.2X SSC) for 15 minutes and incubated with prehybridization buffer (40% formamide in 0.2X SSC) for 20 minutes at 43°C in a humified incubation tray. Following replacement with (CAG)6CA-5' Texas red-labeled 2-Omethyl RNA 20-mers probe in hybridization buffer (1:1000, 10% dextran sulfate and 40% formamide in 0.2X SSC), cells were incubated at 37°C overnight. FISH performed with ecc43 cells involved differently formulated wash buffer (10% formamide in 2X SSC), prehybridization buffer (40% formamide in 2X SSC),

and hybridization buffer (10% dextran sulfate and 40% formamide in 2X SSC). The cells were washed twice with wash buffer for 15 minutes at 37°C and stained with mounting media with DAPI. The cells were imaged with an EVOS fluorescence microscope at 10X and 40X magnification.

RT-PCR for RNA splicing analysis

RNA splicing variants were determined by RT-PCR. Briefly, total RNAs were purified from cells using Direct-zol RNA Miniprep Kits (Zymo Research) with DNaseI treatment. Complementary DNA was synthesized with iScript™ cDNA Synthesis Kit (Biorad). Taq DNA Polymerase with Standard Taq Buffer (NEB) was used for PCR. After agarose electrophoresis with ethidium bromide, the gel images were obtained by Azure Biosystems™ c280 (Azure Biosystems). The intensity of the bands was measured with Image J (reference, https://pubmed.ncbi.nlm.nih.gov/22930834/). We used the following primers:

MBNL1 forward; 5'- TCAAGGCTGCCCAATACCAG-3',

Reverse; 5'-TGTTGGCTAGAGCCTGTTGG-3'.

ADD3 forward; 5'- ACCAGCTCCTCCTAACCCAT-3',

Reverse; 5'-GCCTTCAGGTGACAGGACTT-3'.

RESULTS

Development of nuclear OptiDicer

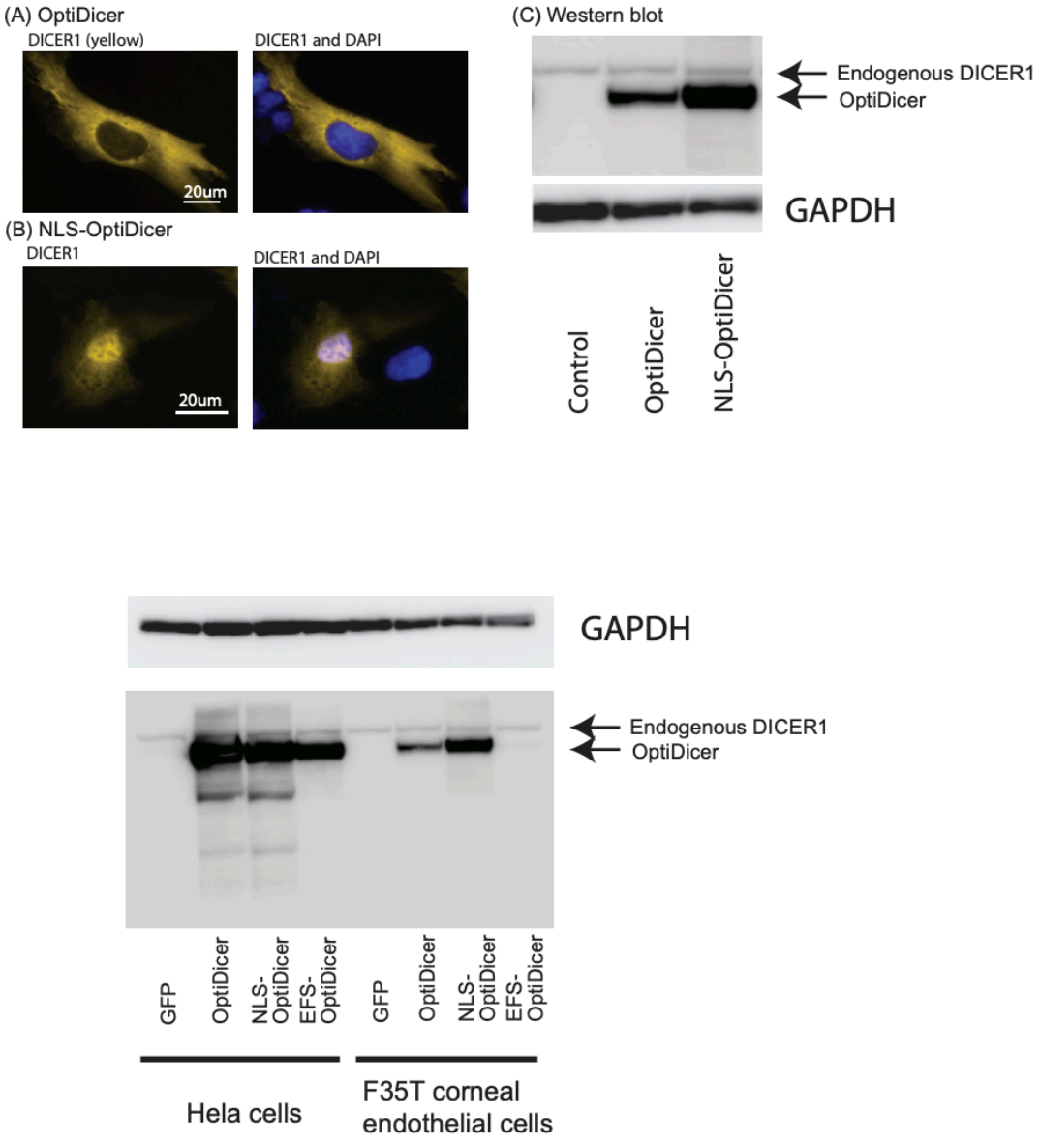

GFP, OptiDicer and NLS-OptiDicer have the same promoter (CMV).
EFS-OptiDicer has a different promoter (EFS) which is weaker than the CMV promoter.
Hela cells did not get affected so much, but F35T did.

Fig. 5: 40x immunofluorescence and western blot gel images showing DICER1, OptiDicer, and NLS-OptiDicer expression in F35T cells and control Hela cells.

As demonstrated in Fig. 5A, OptiDicer (yellow fluorescence) is mainly expressed in the cell cytosol. In the F35T cells, we were unable to detect endogenous DICER1 by immunofluorescence. DICER1 is generally localized to the cytosol but is also present in the nucleus. To target nuclear CUG RNA, we introduced a nuclear localization signal (NLS, SV40) at the N-terminus (NLS-OptiDicer, Fig. 5B). Although NLS-OptiDicer is still expressed in the cytosol, it is expressed efficiently in the nucleus as demonstrated by the colocalization of DAPI staining (blue) and NLS-OptiDicer expression (yellow fluorescence). In Fig. 5C, we confirmed the protein level expression of DICER1, OptiDicer, and NLS-OptiDicer in F35T cells by western blot with GFP and EFS-OptiDicer controls. NLS-OptiDicer showed efficient protein expression greater than DICER1 expression, and equivalent or more than OptiDicer1 expression.

NLS-OptiDicer reduced CUG-RNA accumulations in the nucleus

A

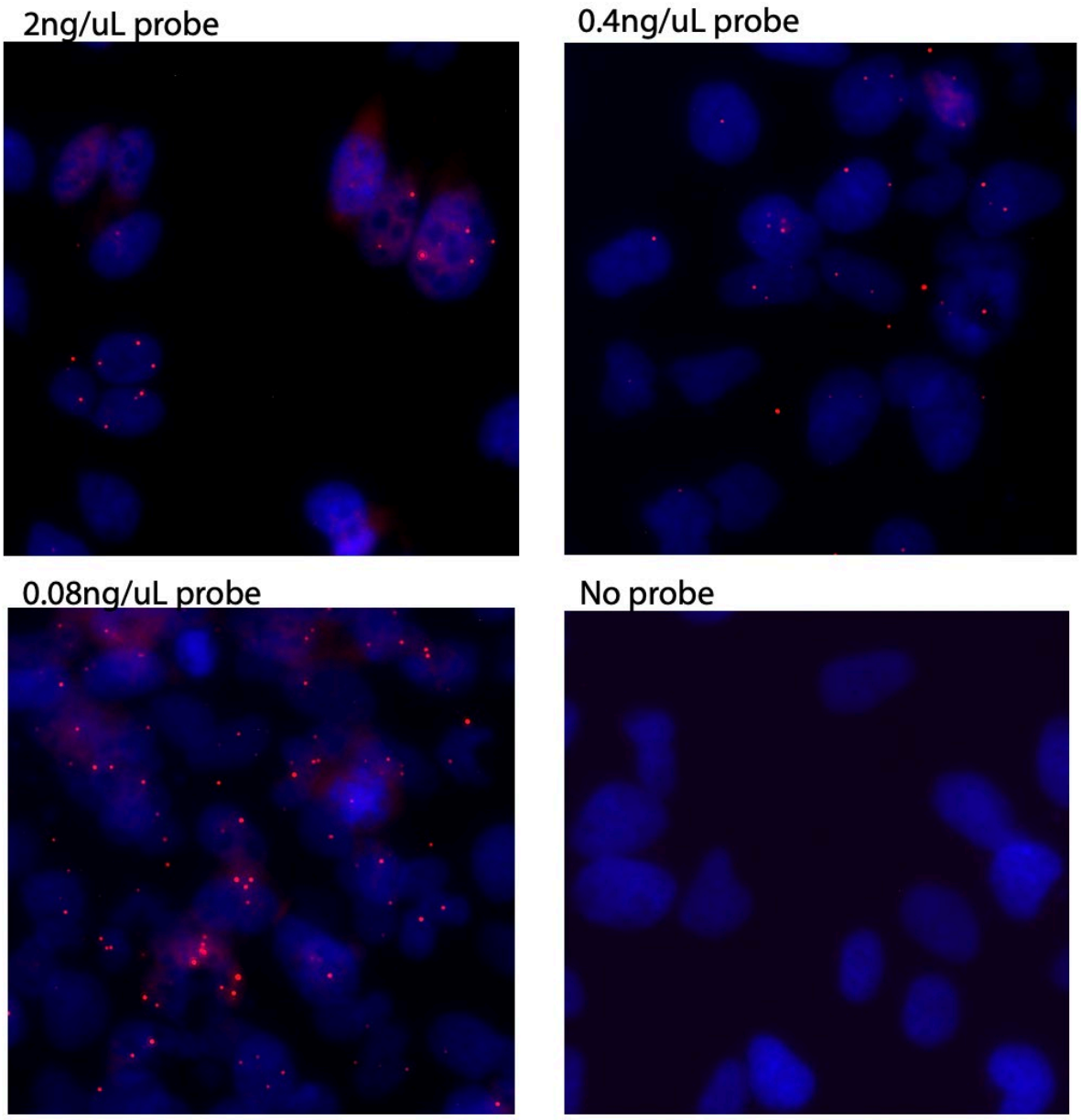

B

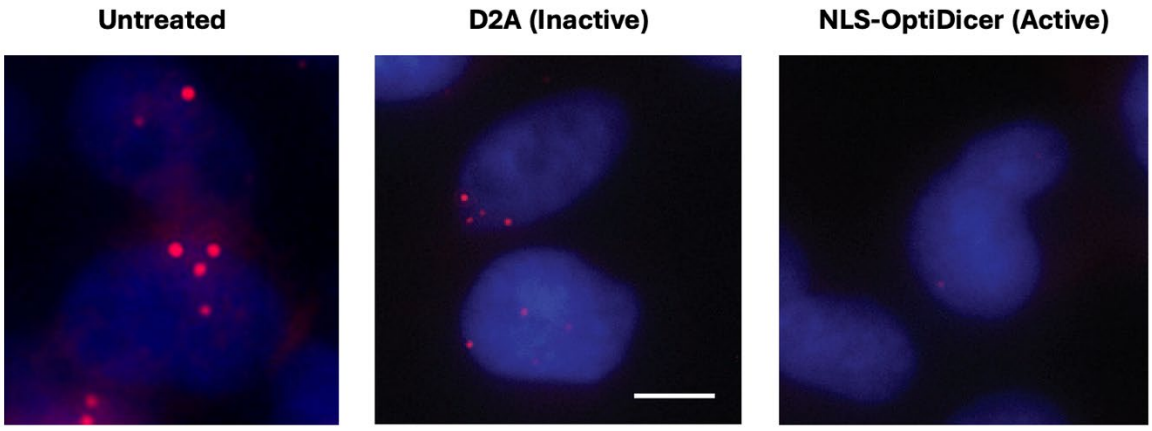

Fig. 6: FISH visualization of CUG RNA foci in F35T cells. A, (CAG)6- CA-5′ Texas red-labeled 2-Omethyl RNA 20-mers probe concentration assay. B, NLS-OptiDicer and D2A control transfection and untreated control with 0.08 ng/uL RNA probe.

Next, we examined whether OptiDicer overexpression can reduce CUG-RNA accumulation (red fluorescence) in F35T cells (nuclei stained DAPI blue). We performed a concentration assay and determined an optimized RNA 20-mers probe concentration of 0.08 ng/uL (Fig. 6A). 0.08 ng/uL of probe was dispensed in FISH experiments with OptiDicer transfected, D2A-OptiDicer transfected, and untreated F35T cells (Fig. 6B). In this experiment, we used D2A-OptiDicer as a control and NLS-OptiDicer experimentally (Fig. 6B). The transfection efficiency was estimated as 50%. We did not find significant cell loss by pCMV-NLS-OptiDicer or pCMV-D2A-OptiDicer transfection. Accumulation of CUG RNA was counted in 276 OptiDicer transfected and 222 D2A-OptiDicer transfected F35T cells. The average number of CUG RNA accumulation was 1.9 +/- 1.4 in OptiDicer-F35T and 2.9 +/- 1.7 in D2A-OptiDicer control F35T ($p = 1.28E-11$), respectively. In comparison, the average number of CUG RNA accumulations counted in 17 untreated F35T cells was 2.5 +/- 1.1 ($p = 0.045$).

NLS-OptiDicer shifts RNA splicing

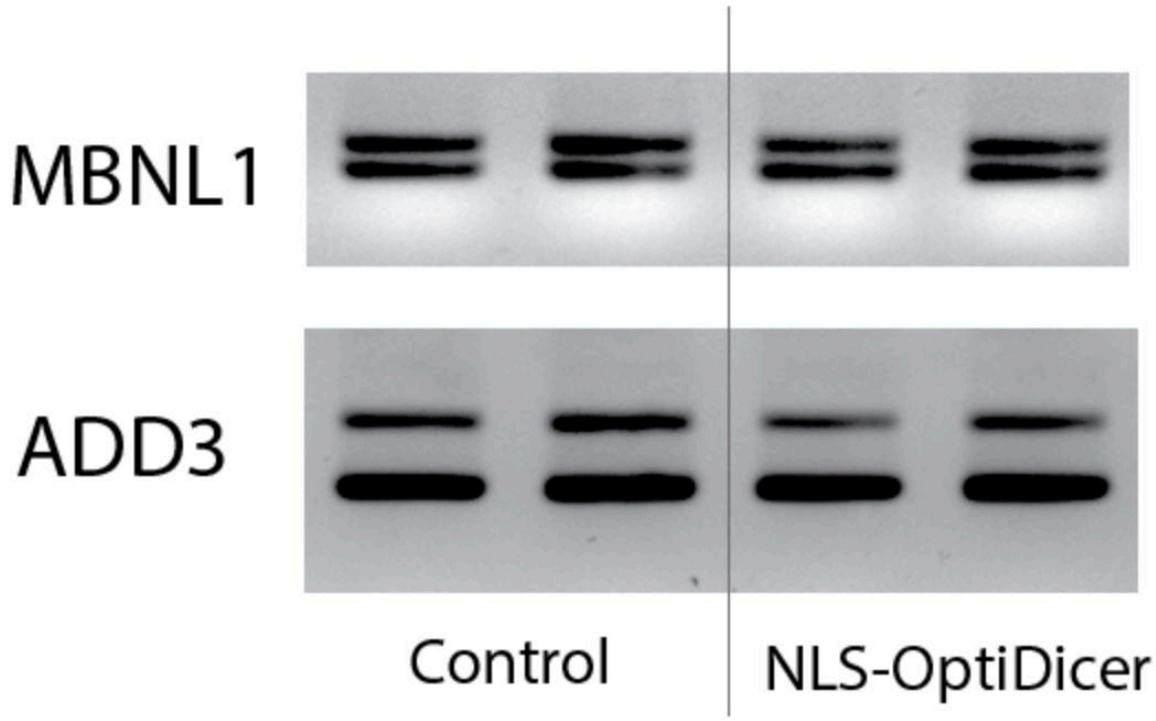

Fig. 7: RT-PCR gel images showing splicing of MBNL1 and ADD3 with NLS-OptiDicer transfection in F35T cells and control corneal endothelial cells.

Finally, we investigated whether NLS-OptiDicer shifts RNA splicing of MBNL1 and ADD3 in F35T cells. MBNL1 and ADD3 are genes previously identified as being influenced by mutant TCF4. We observed alteration of splicing in the genes with transfection of NLS-OptiDicer. When compared to RT-PCR gels of untreated F35T cells, we found that NLS-OptiDicer expression modified the band intensity of exons included in F35T cells. The band intensity of exons qualified in the RT-PCR gel images was measured with ImageJ. The ratio of the upper band intensity to the lower band for MBNL1 was calculated to be 0.90 +/ 0.06 for the control and 0.63 +/- 0.03 for NLS-OptiDicer. For ADD3, the ratio of the upper band intensity to the lower band for ADD3 was calculated to be 0.23 +/- 0.03 for the control and 0.17 +/- 0.02 for NLS-OptiDicer.

DISCUSSION

We found that OptiDicer significantly decreased CUG-RNA accumulation in late-onset FECD patient derived corneal endothelial cells (F35T) from 2.9+/-1.7 foci per cell to 1.9+/-1.4 foci per cell. Our results also indicated that NLS-OptiDicer expression shifts alternative splicing of MBNL1 and ADD3 in F35T cells. While OptiDicer had robust expression in immunofluorescent images and western blot gel images, transfection efficiency was approximated to be only 50% (i.e., only 50% of cells expressed the GFP tag). This low transfection efficiency may underestimate the therapeutic effect of OptiDicer.

We did not include our experimentation with the FECD cell lines ecc20 and ecc43 in this report. In contrast to F35T, transfection efficiency for ecc20 and ecc43 was approximated to be 30-40%. The low transfection efficiency made it impossible to yield significant results with immunofluorescence, western blot, and RT-PCR data. All three cell lines mentioned are derived from late-onset Fuchs' dystrophy patients. The age of the donor renders the cell line more susceptible to mutation. In addition, corneal endothelial cells are difficult to culture in regard to maintaining their phenotypes. These factors may contribute to low transfection efficiency and failure to replicate the results found in F35T with other FECD cell lines.

Future studies will explore OptiDicer in other cell lines from FECD patients (e.g., ecc20 and ecc43) with improved transfection methods. I began the process of optimizing OptiDicer transfection by performing AAV incubation and electroporation with a Nucleofector™ machine. Further experimentation with these methods may increase OptiDicer transfection efficiency to our target of 80-100%. However, our current results preliminarily suggest that OptiDicer can be a potential treatment for long CUG RNA repeat FECD.

Bibliography

Aiello, Francesco et al. “Global Prevalence of Fuchs Endothelial Corneal Dystrophy (FECD) in Adult Population: A Systematic Review and Meta-Analysis.” Journal of ophthalmology vol. 2022 3091695. 14 Apr. 2022, doi:10.1155/2022/3091695

Berry, Garrett Edward, and Aravind Asokan. “Cellular transduction mechanisms of adeno-associated viral vectors.” Current opinion in virology vol. 21 (2016): 54-60. doi:10.1016/j.coviro.2016.08.001

Du, Jintang, et al. “RNA Toxicity and Missplicing in the Common Eye Disease Fuchs Endothelial Corneal Dystrophy.” *Journal of Biological Chemistry*, vol. 290, no. 10, Mar. 2015, pp. 5979–5990, doi:10.1074/jbc.m114.621607.

Elsa Prudent, Didier Raoult, Fluorescence in situ hybridization, a complementary molecular tool for the clinical diagnosis of infectious diseases by intracellular and fastidious bacteria, FEMS Microbiology Reviews, Volume 43, Issue 1, January 2019, Pages 88–107, https://doi.org/10.1093/femsre/fuy040

Faye, Pierre Antoine, et al. “Focus on Cell Therapy to Treat Corneal Endothelial Diseases.” *Experimental Eye Research*, vol. 204, Mar. 2021, p. 108462, doi:10.1016/j.exer.2021.108462.

Hamill, Cecily E et al. “Fuchs endothelial cornea dystrophy: a review of the genetics behind disease development.” Seminars in ophthalmology vol. 28,5-6 (2013): 281-6. doi:10.3109/08820538.2013.825283

Haschek, W. M., Rousseaux, C. G., Wallig, M. A., & Alden, C. L. (2002). Handbook of toxicologic pathology. Academic Press.

Jurkunas, Ula V., et al. “Evidence of Oxidative Stress in the Pathogenesis of Fuchs Endothelial Corneal Dystrophy.” *The American Journal of Pathology*, vol. 177, no. 5, Nov. 2010, pp. 2278–2289, doi:10.2353/ajpath.2010.100279.

“LOXHD1 Lipoxygenase Homology PLAT Domains 1 [Homo Sapiens (Human)] Gene ID: 125336, Updated on 7-Apr-2024 Download Datasets.” *National Library of Medicine*.

Ma, Enbo, et al. “Autoinhibition of Human Dicer by Its Internal Helicase Domain.” *Journal of Molecular Biology*, vol. 380, no. 1, June 2008, pp. 237–243, doi:10.1016/j.jmb.2008.05.005.

Matthaei M, Hribek A, Clahsen T, Bachmann B, Cursiefen C, Jun AS. Fuchs Endothelial Corneal Dystrophy: Clinical, Genetic, Pathophysiologic, and Therapeutic Aspects. Annu Rev Vis Sci. 2019 Sep 15;5:151-175. doi: 10.1146/annurev-vision-091718-014852. PMID: 31525145.

Mathews, Priya, et al. “2022 EYE Banking Statistical Report—Executive Summary.” *Eye Banking and Corneal Transplantation*, vol. 2, no. 3, 15 Aug. 2023, doi:10.1097/ebct.0000000000000008.

Mootha, V Vinod et al. “TCF4 Triplet Repeat Expansion and Nuclear RNA Foci in Fuchs' Endothelial Corneal Dystrophy.” Investigative ophthalmology & visual science vol. 56,3 2003-11. 26 Feb. 2015, doi:10.1167/iovs.14-16222

Mootha, V Vinod et al. “Fuchs' Endothelial Corneal Dystrophy and RNA Foci in Patients With Myotonic Dystrophy.” Investigative ophthalmology & visual science vol. 58,11 (2017): 4579-4585. doi:10.1167/iovs.17-22350

Nanda, Gargi Gouranga, and Debasmita Pankaj Alone. “REVIEW: Current understanding of the pathogenesis of Fuchs' endothelial corneal dystrophy.” Molecular vision vol. 25 295-310. 5 Jun. 2019

Rong, Ziye et al. “Trinucleotide Repeat-Targeting dCas9 as a Therapeutic Strategy for Fuchs' Endothelial Corneal Dystrophy.” Translational vision science & technology vol. 9,9 47. 31 Aug. 2020, doi:10.1167/tvst.9.9.47

Rosenblum P, Stark WJ, Maumenee IH, Hirst LW, Maumenee AE. Hereditary Fuchs' Dystrophy.
Am J Ophthalmol. 1980 Oct;90(4):455-62. doi: 10.1016/s0002-9394(14)75011-1. PMID: 6968504.

Sarnicola C, Farooq AV, Colby K. Fuchs Endothelial Corneal Dystrophy: Update on Pathogenesis and Future Directions. Eye Contact Lens. 2019 Jan;45(1):1-10. doi: 10.1097/ICL.0000000000000469. PMID: 30005051.

Sheerin, Angela N., et al. “Characterization of Cellular Senescence Mechanisms in Human Corneal Endothelial Cells.” *Aging Cell*, vol. 11, no. 2, 29 Dec. 2011, pp. 234–240, doi:10.1111/j.1474-9726.2011.00776.x.

Soh YQ, Peh GS, Mehta JS. Evolving therapies for Fuchs' endothelial dystrophy. Regen Med. 2018 Jan;13(1):97-115. doi: 10.2217/rme-2017-0081. Epub 2018 Jan 23. PMID: 29360003.

Wang, Xiaowei. “Composition of Seed Sequence Is a Major Determinant of Microrna Targeting Patterns.” *Bioinformatics*, vol. 30, no. 10, 26 Jan. 2014, pp. 1377–1383, doi:10.1093/bioinformatics/btu045.

Wieben, Eric D., et al. “A Common Trinucleotide Repeat Expansion within the Transcription Factor 4 (TCF4, E2-2) Gene Predicts Fuchs Corneal Dystrophy.” *PLoS ONE*, vol. 7, no. 11, 21 Nov. 2012, doi:10.1371/journal.pone.0049083.

Wieben, Eric D., Ross A. Aleff, Xiaojia Tang, et al. “Trinucleotide Repeat Expansion in the Transcription Factor 4 (*Tcf4*) Gene Leads to Widespread Mrna Splicing Changes in Fuchs’ Endothelial Corneal Dystrophy.” *Investigative Opthalmology & Visual Science*, vol. 58, no. 1, 24 Jan. 2017, p. 343, doi:10.1167/iovs.16-20900.

Xing, Chao, et al. “Transethnic Replication of Association of CTG18.1 Repeat Expansion of*Tcf4*Gene with Fuchs’ Corneal Dystrophy in Chinese Implies Common Causal Variant.” *Investigative Opthalmology & Visual Science*, vol. 55, no. 11, 7 Nov. 2014, p. 7073, doi:10.1167/iovs.14-15390.

Zhang J, Patel DV. The pathophysiology of Fuchs' endothelial dystrophy--a review of molecular and cellular insights. Exp Eye Res. 2015 Jan;130:97-105. doi: 10.1016/j.exer.2014.10.023. Epub 2014 Nov 1. PMID: 25446318.